Journal Name

ARTICLE TYPE

Cite this: DOI: 10.1039/xxxxxxxxxx

Interaction of Testosterone-Based Compounds with Dodecyl Sulphate Monolayers at the Air-Water Interface†

Daniel T. Allen,[a] Nikou Damestani,[a] Yussif Saaka, [b] M. Jayne Lawrence [c] and Christian D. Lorenz *[a]

Received Date
Accepted Date

DOI: 10.1039/xxxxxxxxxx

www.rsc.org/journalname

A series of atomistic molecular dynamics simulations investigating the interactions between three different testosterone-based compounds (testosterone (T), testosterone propionate (TP) and testosterone enanthate (TE)) and sodium dodecyl sulphate (SDS) and ammonium dodecyl sulphate (ADS) monolayers, which vary only in the sodium or ammonium counterions used to neutralise the sulphate headgroup. These simulations were used to investigate how the structural and interfacial properties of the monolayer was affected by changing the number of drug molecules present per monolayer, and the chemical nature of the surfactant counterions and the testosterone-based compounds. Our results show that the structure of the interfacial water layer is affected by the change of the counterion but not the chemistry of the drug molecules. As a result of the difference in their chemical structure, the T, TP and TE drug molecules take different locations and orientations within the monolayers. Finally, we observed that the hydration of the drug molecules encapsulated within the ADS monolayers is significantly less than when they are encapsulated within the SDS monolayers. Understanding the role that the counterion and the chemistry of the drug molecules in these systems provides us with a detailed description of the interactions that cause ADS micelles to encapsulate significantly less drug molecules than SDS micelles, which we have recently observed experimentally.

1 Introduction

The unique chemical structure of surfactants enables them to form a variety of self-assembled structures including monolayers at the air-water interface and micelles, vesicles and bilayers in solution. The ability to form these complex nanostructures allows surfactants to be used in the production of novel pharmaceutical, food and personal care products, material recovery processes, and environmental remediation [1–15]. In all of these applications, the hydrophobic interior of the aggregate structures can be used to solubilise other slightly soluble nonpolar substances.

While surfactants are widely applied in the formulation of drug delivery vehicles, the understanding of how the molecular structures of surfactants and drug compounds affect the drug-surfactant interactions and therefore the solubilisation of the drugs into aggregates of the surfactant is still quite limited. In general, it is understood that the solubilisation of a drug depends on the hydrophobic interactions between the drug and surfactant molecules, while hydrophilic and electrostatic interactions of the drug molecules will affect their location within the aggregates [16,17]. While this understanding of the basic interactions that govern the behaviour of surfactant-based drug formulations is useful, it is not enough to attempt to optimise the composition of a formulation to maximise the encapsulation and stability of an aggregate. Therefore there is a significant interest in generating a more detailed understanding on how the surfactant-drug interactions and the interactions of the surfactant and drug with the solvent phase affect the solubilisation and structure of the micelle, which in turn can be used to optimise its drug delivery properties.

Molecular dynamics (MD) simulations are a powerful tool that have the capability to provide detailed information regarding the interactions which govern the encapsulation process of small molecules into self-assembled aggregates of surfactants. As a re-

[a] Biological Physics & Soft Matter Group, Department of Physics, King's College London, London WC2R 2LS, United Kingdom. E-mail: chris.lorenz@kcl.ac.uk
[b] Pharmaceutical Biophysics Group, Institute of Pharmaceutical Science, Franklin-Wilkins Building, King's College London, 150 Stamford Street, London SE1 9NH, United Kingdom.
[c] Division of Pharmacy and Optometry, School of Health Sciences, Stopford Building, The University of Manchester, Oxford Road, Manchester M13 9PT, United Kingdom.

† Electronic Supplementary Information (ESI) available: Plots of the distribution of water molecules around (a) the DS^- head groups in the various systems (b) the oxygen atoms in the different testosterone-based compounds and (c) the distribution of cations around the oxygen atoms in the different testosterone-based compounds. See DOI: 10.1039/b000000x/

sult there have been used in several investigations of the solubilisation of small molecules in surfactant micelles[1,18–21,21–25]. Meanwhile, there has been a wealth of scientific research using MD simulations to gain a similar understanding of the molecular-scale interactions that govern the interfacial properties of the surfactants and the self-assembled structures that they form at the air/water interface[26–38]. However, very little has been done with simulations investigating the interactions of drug molecules with surfactant monolayers, and the research that has been done primarily focusses on the interaction of drug molecules with lipid monolayers[39–43]. Experimentally, the best way of gaining information on the amount of drug incorporated into a monolayer and the resulting location of the drug within a monolayer is specular neutron reflectivity (SNR). However, as is the case with MD simulations, very little research has been reported on the interactions of small molecules and surfactant monolayers. The experimental investigations that have been reported were focussed on oil[44,45] and fragrance[46,47] molecules. Only recently have we reported an interdisciplinary investigation of a drug molecule with a SDS monolayer[48].

In this study, we used classical MD simulations to investigate the interactions between three different testosterone-based compounds (testosterone (T), testosterone propionate (TP) and testosterone enanthate (TE)) and sodium dodecyl sulphate (SDS) and ammonium dodecyl sulphate (ADS) surfactants, which vary only in the sodium or ammonium counterions used to neutralise the sulphate headgroup (see Fig. 1 for molecular structures). The position, orientation and hydration of the three testosterone-based compounds were investigated within monolayers of each surfactant. As surfactant monolayers and micelles are in thermodynamic equilibrium with one another and both exist in experimental systems when the concentration of surfactants within the system is above the critical micelle concentration (cmc), then the structural and interfacial properties of the monolayers studied here will be related to those in a micelle. The results of this investigation provide a detailed understanding of the interactions that result in the reduced encapsulation of testosterone-based compounds in ADS micelles as compared to their encapsulation in SDS micelles[49]. Additionally, these results provide an insight into how modifying the chemistry of drug molecules and the molecules used to encapsulate them can affect the positioning of the molecules within the drug delivery vehicle.

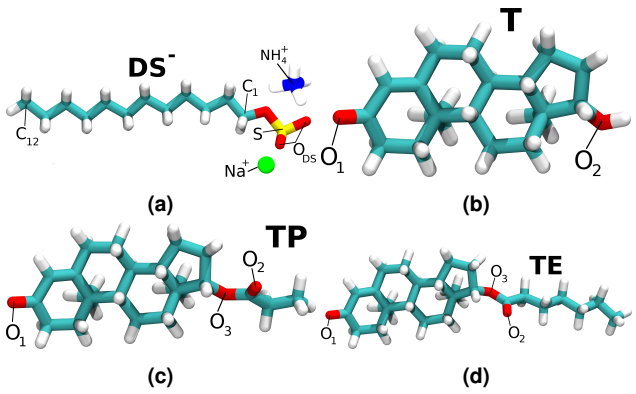

Fig. 1 The chemical structures of: a) DS^- with Na^+ and NH_4^+ counterions, b) T, c) TP, d) TE. In these figures, the colours cyan, white, red, yellow, green and blue are used to represent the elements: carbon, hydrogen, oxygen, sulphur, sodium and nitrogen respectively.

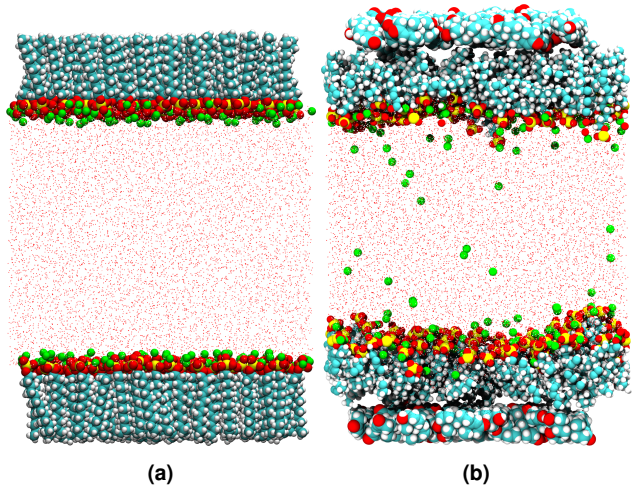

Fig. 2 Initial configurations of (a) the SDS monolayer system and (b) the SDS monolayer system with testosterone molecules. The colours cyan, white, red, yellow and green are used to represent the elements: carbon, hydrogen, oxygen, sulphur and sodium respectively. In (b), the testosterone molecules are visible in the vacuum regions both above and below the respective monolayer leaflets.

2 Model and Methodology

2.1 Simulated systems

All-atom MD simulations were used to investigate the structural and interfacial properties of ADS and SDS surfactant monolayers at the air/water interface with different counterions. Each of these monolayer systems were comprised of two monolayer leaflets separated by a 60 Å thick water slab, which ensured that the electrostatic interactions from one monolayer were not felt by the other monolayer. The resulting water slab consists of 9600 water molecules with a density of 1 g/ml.

The initial structures of the DS^- monolayers, each consisting of 100 DS^- molecules, were built using the Packmol software package[50] and were neutralised by the addition of 100 Na^+/NH_4^+ counterions for the SDS/ADS systems per leaflet, which were placed near the headgroup regions of the DS^- molecules. The simulation box was built with $x-$ and $y-$ dimensions of 69.28 Å each such that the area per surfactant was ~ 48 Å^2. The area per surfactant used in the DS^- monolayer simulations is in agreement with the experimentally determined value for SDS monolayers[51] and was used for all reported monolayers so that the system properties can be fairly compared. Periodic boundary conditions were applied in all dimensions, with the $z-$ dimension of the simulation box set to 200 Å to ensure that the monolayers do not interact with one another through the periodic boundary in the z-axis. The centre of mass of each system was constrained to be at the position $z = 0$ throughout the simulation to make the analysis of the simulation as easy as possible. The initial configuration for the SDS monolayer system is shown in Figure 2a, illustrating the monolayer geometry.

The testosterone-based compounds (testosterone (T), testosterone propionate (TP) and testosterone enanthate (TE)), whose chemical structures are shown in Figure 1, were introduced after the ADS/SDS monolayers were thoroughly equilibrated. The drug molecules were initially placed randomly in the vacuum regions above and below the top and bottom monolayer leaflets respectively in each system, within 5-10 Å of the hydrocarbon tails and oriented such that they were perpendicular to the z-axis, as shown in Figure 2b. The placement of the drug molecules in these regions mimicked the placement of the drugs in the experiments in which n-hexane was used to deliver the drugs onto the hydrocarbon tails of the monolayers. In each case, each drug/monolayer combination was studied with three different numbers of drug molecules per monolayer present: (a) a single drug per monolayer, (b) a number of drugs per lipid that is representative of what is found in the micelles from solubilisation experiments and the fitting of neutron scattering experiments of the same systems[49], and (c) twice the number of drugs per surfactant found in the micelles experimentally.

2.2 Simulation protocol

The same simulation protocol was used for each simulation to study the various systems presented in this manuscript.

First, an energy minimisation was performed on each of monolayer systems using 100 000 steps as the maximum number of force/energy evaluations. Then the minimum energy state was simulated in the NVT ensemble for 10 ns for thermalisation. The ADS and SDS monolayer systems were simulated a further 50 ns in the NVT ensemble to equilibrate the monolayers before the drug molecules were added. Then the final configuration from these equilibration simulations were used to build the systems with the different drug molecules. The drug molecules were placed within 5-10 Å of the terminal methyl groups of the hydrocarbon tails of the DS^- surfactants, and the drug molecules were oriented with their primary axis perpendicular to the z-axis. Finally, these various systems were simulated for a further 50 ns using the NVT ensemble in order to investigate the interations between the testosterone-based compound and the DS^- monolayers.

All of the simulations presented in this manuscript were performed at $T = 300$ K using the LAMMPS simulation package[52] with the CHARMM force field[53,54] for the description of both inter- and intra-molecular interactions of the DS^- molecules, the various counterions and also the testosterone-based compounds[55,56]. The TIP3P water model[57], modified for the CHARMM forcefield[58], was used to describe interactions involving water. This combination of forcefields has previously been shown to give a good description of SDS micelles and DS^- monolayers[1,26,59,60].

The van der Waals interactions were cut-off at 10 Å whilst the electrostatic interactions were cut-off at 12 Å. The PPPM method[61] was used to compute long-range Coulombic interactions. The equilibration and production runs for all monolayer simulations utilised the Nose-Hoover thermostat[62] to fix the system temperature. A timestep of 2 fs was used in all simulations to ensure stable integration of Newton's equations of motion with the velocity Verlet algorithm whilst all hydrogen-containing bonds were constrained using the SHAKE algorithm[63]. All of the measurements reported in this manuscript were conducted using the last 10 ns of the production simulations, during which the position of the drug molecules within the monolayers and the orientation of the surfactant molecules was observed to not be changing significantly.

2.3 Analysis of simulation trajectories

2.3.1 Constructing an intrinsic surface for a surfactant monolayer

Developing a description of the interfacial behaviour and structure of surfactant aggregates is crucial to understanding their function for many different processes. Physical properties such as size, geometry/shape, hydrophobicity and roughness all have an affect on the observed behaviour of aggregates and are largely influenced by the surface properties. It is therefore of vital importance that a thorough and careful treatment of the interfaces of these structures be incorporated into analysis.

For a system comprising of two distinct phases, the *intrinsic surface*, denoted by $\xi(\mathbf{R}) = \xi(x,y)$, is defined as the location in which one phase comes in contact with the other. In general, the intrinsic surface is constructed from a finite number of anchor points: atoms which are deemed to be at the interfacial region. For DS^- monolayers, the sulphur atoms in the DS^- head groups are generally used as the anchor points, as they will generally be found near the monolayer/water interface.

There are a number of different ways to construct the intrinsic surface for liquid interfaces reported in the literature. For computational efficiency, the algorithm proposed by Berkowitz *et al*[64] was employed in this manuscript to determine the intrinsic surface of the DS^- monolayers, as it was employed previously to investigate the interaction of various counterions with DS^- surfactants[26]. In essence, this method is performed by projecting the location of a particle of interest and the anchor points used to define the interface onto the x-y plane. Next, the closest anchor point to the particle of interest within this projected two-dimensional representation is established. Finally, the location of the intrinsic surface for the particle of interest is assigned the value of the z-coordinate of the closest anchor point.

2.3.2 Determination of the intrinsic density

In the DS^- monolayer systems, the intrinsic density is used to describe the average density of different atomic species as a function of their distance away from the intrinsic surface. The intrinsic density provides a description of the interfacial structure of the various atomic components in the system such as counterions, solvent and drug molecules. The intrinsic density is particularly useful for describing the structure of water molecules in the vicinity of the interface, which is known to strongly impact the ability of solutes to penetrate through the monolayer surface.

The intrinsic density of a given atomic species is defined math-

ematically as:

$$\widetilde{\rho}(z) = \left\langle \frac{1}{A_0} \sum_{i=1}^{N} \delta(z - z_i + \xi(\mathbf{R_i})) \right\rangle \quad (1)$$

where the summation indexed by i runs over all N particles of a given atomic species, $\xi(\mathbf{R_i})$ represents the *intrinsic surface* for a given configuration, $\mathbf{R_i} = (x_i, y_i)$ is the location of particle i in the x-y plane for a given configuration and A_0 is the cross sectional area of the interface. The z-coordinate of the i^{th} particle is denoted by z_i and z represents the vertical distance from the DS^-/water interface to particle i where values of $z > 0$ and $z < 0$ represent locations within the water slab and towards the vacuum region respectively.

2.3.3 Measurement of monolayer structural properties

A detailed description of the monolayer structure has been achieved by calculating different quantities to study how monolayer structure changes with the addition of testosterone-based compounds. In the following paragraphs, these quantities are explained in detail.

The thickness of the DS^- monolayers provide insight into how the surfactants arrange and orient themselves within the monolayer. In this manuscript, the thickness of the hydrocarbon tail d_{tail} and the head group d_{head} of the surfactants have been determined. The thickness of the hydrocarbon tail was determined by taking the difference between maximum and minimum values of the z-coordinates of the carbons in the tails of each DS^- molecule. Then the value of d_{head} is determined by averaging over all molecules in all configurations.

Meanwhile, the instantaneous *thickness of the headgroup region* of the DS^- monolayer is calculated in a similar manner as the tail thickness and can be used to monitor how the head group region is affected as the composition of drug molecules changes. The thickness of a headgroup in a given DS^- molecule is determined by first establishing the maximum and minimum z-coordinates of the four oxygen atoms in the headgroup, and then taking the difference between the maximum and minimum of these z-values. Then to find the thickness of the headgroup region of a monolayer d_{head}, this distance is averaged over all DS^- molecules in every snapshot.

The *monolayer interfacial roughness* can strongly influence the ability of solutes to penetrate through the monolayer surface. The interfacial roughness is described by the value of the root-mean-squared deviation (RMSD) for the difference between the z-coordinate of a sulphur atom in the DS^- headgroup and the mean value of the z-coordinates of all sulphur atoms present in a monolayer within a given configuration of the trajectory: $|z_i - z_{\text{avg}}|$.

The structure of the DS^- molecules within the monolayers can also be described via different geometric measures of the molecules. For example, the surfactant chain tilt angle, θ_t, is defined as the angle between the vector formed between the C_1 atom (the carbon nearest the head group) and the C_{12} atom (the terminal carbon of the hydrocarbon chain) and a unit vector in the z-direction. When this angle is zero, the hydrocarbon tail is parallel to the z-axis and when this angle is 90°, the DS^- molecule is lying in the x-y plane. Additionally, the surfactant headgroup tilt angle, θ_h, was also investigated for all of the monolayer systems and is defined as the angle between the vector formed between S (the sulphur atom in the DS^- headgroup) and C_1 atoms, and the vector formed between C_1 and C_{12} atoms. When this angle is zero, the entire molecule is aligned linearly and when this angle is 90° the headgroup is oriented such that it is perpendicular to the DS^- hydrocarbon chain. In both cases, these angles are averaged every molecule in a configuration and over all configurations that were analysed.

The surface tension of the surfactant monolayers loaded with drug molecules is calculated direclty for each system. The monolayer surface tension (γ_m) is determined from the difference between the normal (P_N) and lateral (P_L) pressures as shown:

$$\gamma_m = \left\langle (P_N - P_L) \times (L_z/2) \right\rangle, \quad (2)$$

where L_z is the box size in the direction normal to the monolayer interfaces. As the normal is oriented along the z-axis in our systems, the lateral pressure P_L is the average of the pressure in the x- (P_{xx}) and y-directions (P_{yy}): $P_L = (P_{xx} + P_{yy})/2$. The values of γ_m reported here are calculated and then averaged over 10 ns of the production simulation.

2.3.4 Position and Orientation of Testosterone Compounds

The preferred position and orientation of drug molecules within surfactant aggregates has profound implications on the nature of their encapsulation properties. These may be affected by the chemical nature of the drug and also the physical characteristics of the surfactant species itself, such as the choice of counterion and hydrophobic tail length. The orientation of drug molecules is described by the cosine of the angle formed between the vector pointing from the O_2 atom to the O_1 atom (see Figure 1) in the drug molecule and the unit vector: (0,0,1) or (0,0,-1) for drug molecules in the top or bottom monolayer leaflets respectively. When $\cos(\theta)$ is equal to -1, the entire drug molecule is aligned parallel to the z-axis with the O_2 atom nearest the vacuum region and the O_1 atom nearest the water slab, when $\cos(\theta)$ is equal to 0 the drug molecule is oriented in the x-y plane and when $\cos(\theta)$ is equal to 1, the drug molecule is again aligned parallel to the z-axis but with the O_1 atom nearest the vacuum region and the O_2 atom nearest the water slab.

The location of a drug molecule is used to determine how deep a drug molecule is inserted into the monolayer and is defined as the midpoint of the vector connecting the O_1 and O_2 atoms (v_{O_1,O_2}). In this case, the orientation distributions are calculated as a function of the distance that the drug molecule is away from the intrinsic surface of the monolayer into the hydrocarbon tail region. The space amongst the surfactant monolayers has been divided into four distinct regions: Headgroup, C_{1-4}, C_{5-8} and C_{9-12}. These regions are determined by first determining the surfactant molecule which is closest in the x-y plane. Then the z-coordinates of the atoms in the surfactant molecule were used to define these four regions, and the z-coordinate of v_{O_1,O_2} was used to identify which region the drug molecule resided in. It should be noted that the size of these regions will vary as the tilt angle of

the individual surfactant chains vary, but this method is consistent with identifying an intrinsic surface at the four different levels and mapping it out across the monolayers and using these surfaces as criteria for identifying the location of the drug molecule as is done for the solvent phase in reference to the monolayer surface.

3 Results

In this section, the results of the previously described analyses are presented for the SDS and ADS monolayers with each of the three different testosterone derivatives.

3.1 Monolayer intrinsic density

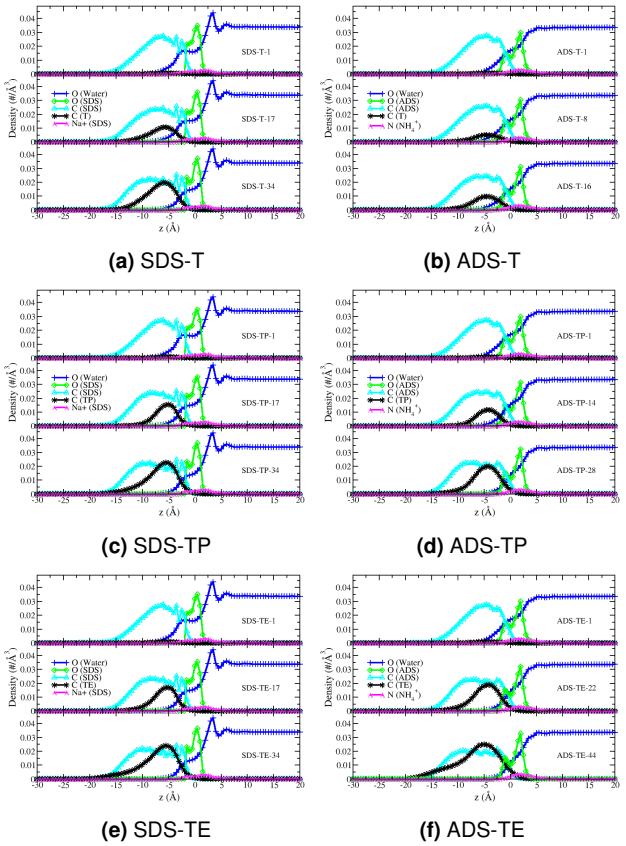

(a) SDS-T **(b)** ADS-T **(c)** SDS-TP **(d)** ADS-TP **(e)** SDS-TE **(f)** ADS-TE

Fig. 3 Intrinsic density profiles for the monolayer simulations. The colours green, blue and magenta are used to depict the density of DS^- elements: oxygen, carbon, and sodium/nitrogen in the counterions respectively. The colours blue and black depict the density of oxygen atoms in water and carbon atoms in the testosterone-based molecules respectively. (Note: the errors on these measurements are smaller than the size of the symbols used to represent them.)

Intrinsic density profiles, shown in Figure 3, provide a detailed characterisation of the interfacial water structure and the location of testosterone-based compounds within the monolayers. One significant distinction between these plots for SDS and ADS monolayers is the density profiles of oxygen atoms in water molecules, O_W, as shown by the blue curves in Figure 3. At smaller values of z, corresponding to the monolayer interfacial region, the SDS monolayers exhibit two distinct density peaks. The largest peak is situated at $z = 3.5$ Å whilst the smaller peak is located at $z = 6$ Å which indicates that there are two interfacial water layers near the SDS headgroups. For the ADS monolayers, the structure of water molecules in the interfacial region is quite different. Rather than exhibiting peaks, the density of O_W atoms remains constant at the bulk value and it begins to decrease monotonically from the headgroup region for some distance inside the monolayer hydrocarbon tail region ($z < 0$). Therefore, the water is less ordered at the interface of the ADS monolayers than the SDS monolayers, which is consistent with what we observed when studying DS^- monolayers with different counterions in the absence of drug molecules[26]. Therefore, the effect of changing the type and the number of drug molecule present within the monolayers has a negligible effect on the interfacial water density, whereas changing the counterion species has a large effect.

Within the monolayer hydrocarbon tail region, $z < 0$, the water density decays and eventually reaches zero in all systems. For the SDS monolayers with 1 drug molecule present, there is a small peak in the density of the O_W atoms located at approximately $z = -3$ Å, which is where the hydrocarbon tails merge with the SDS head group (as $z = -3$ Å is the location where the density of the oxygens in the SDS headgroup and the density of the carbons in the SDS tails overlap). For the SDS systems, this water density peak within the monolayer becomes less prominent as more drug molecules are present, thus the addition of drug molecules results in the expulsion of water from this region of the monolayer. Additionally, none of the ADS monolayers have appreciable density peaks for O_W atoms within the monolayers.

The amount of water within each monolayer n_{H_2O} was calculated for all systems by integrating the intrinsic density of O_W atoms over z from $-\infty \rightarrow 0$, which therefore provides a measure of the average number of water molecules contained within the monolayer interior per unit area. The values for n_{H_2O} are shown in Table 1 & 2 for the SDS and ADS monolayers, respectively. These values reveal that as the number of drug molecules present per monolayer increases, the value of n_{H_2O} decreases for all of the systems. As the monolayers become more densely packed by the addition of drug molecules, water is forced into the bulk water region where it can form more favourable interactions than in the monolayer tail region. The ADS monolayers contain significantly less water within their tail regions. For example, the values of n_{H_2O} for SDS-T-1 and ADS-T-1 are 0.16 $Å^{-2}$ and 0.10 $Å^{-2}$ respectively. Similarly, comparing SDS-TP-1, SDS-TE-1 and ADS-TP-1, ADS-TE-1 reveals n_{H_2O} values of 0.15 $Å^{-2}$ and 0.10 $Å^{-2}$ for SDS and ADS respectively. Therefore by changing the counterions from sodium to ammonium, the water contained within the monolayer decreases by 33% which is significant. The amount of water contained within the interior of surfactant aggregates could have a profound effect on their resulting solubilising ability[49].

The intrinsic density profiles of the sodium and ammonium counterions are shown by the magenta curves in Figure 3 and exhibit a single broad density peak around the monolayer interface ($-5 < z < 5$) in all systems. Therefore, the counterions are situated in the vicinity of the interfacial region, which is also confirmed from visual inspection of the simulation trajectories.

The green curves in Figure 3 show the intrinsic density of oxy-

gen atoms in DS^- molecules, O_{DS}, for all of the monolayers. For the SDS monolayers with a small number of drug molecules present, these distributions exhibit a peak located at $z = 0$ Å, and a shelf located just beneath the monolayer surface at $z \sim -1$ Å. As the number of drug molecules is increased, this density distribution splits into two distinct peaks, the largest of which corresponds to the three ionic oxygen atoms in the surfactant head group, whereas the second smaller peak arises due to the oxygen atom which is bonded to the C_1 and S atoms in the surfactant. As more drug molecules are added to the monolayer, the dynamics of the head groups becomes restricted which results in the increased prominence of the two density peaks of O_{DS} atoms. In the ADS monolayers, the O_{DS} intrinsic density profiles show even sharper peaks than those in SDS; however unlike the SDS monolayers, these peaks are unchanged by the addition of more drug molecules. The counterion species is the predominant factor in determining the structure of the monolayer interface, as opposed to the type or number of the testosterone-based compounds present.

The intrinsic density profiles of carbon atoms in DS^- molecules, C_{DS}, are shown by the cyan curves in Figure 3 and represent the surfactant hydrocarbon chains. These density profiles are non-zero in the region from the monolayer interface ($z \sim 0$) to approximately $z = -15$ Å for all of the SDS and ADS monolayer simulations. There is no significant change in the C_{DS} intrinsic density profiles as the counterion species is changed, however as the number of drug molecules present in the monolayer increases, the C_{DS} density profile flattens out to some extent. This effect is most clearly illustrated in the SDS-TE simulations as the number of TE is increased from 1 to 34, but can be seen in all of the different systems.

The intrinsic density of the carbon atoms (C_T, C_{TP} and C_{TE} for T, TP and TE respectively) in the drug molecules is used to determine their location in the monolayers. Figure 3 shows the intrinsic density profiles of the carbon atoms in the testosterone-based compounds. The black curves show that these molecules are located amid the DS^- hydrocarbon tails and not at the interface. As more drug molecules are added, the density peaks remain around approximately the same value of $z \sim -5$ Å whilst the magnitude of the peaks increase slightly as the additional drug molecules accumulate in the same region of the monolayer. In a recent study, we have shown with both neutron reflectivity and MD simulations that TE resides in the same region of the monolayers when the area per surfactant is changed, and only when the concentration of TE becomes super saturated is there a population of drug molecules which are expelled into the vacuum region outside of the monolayers[48].

3.2 Orientation and position of testosterone-based compounds in monolayers

The intrinsic density plots reveal that the testosterone-based compounds are generally situated within the DS^- hydrocarbon tail region. However they do not contain any information about the orientation of these molecules at different positions within the monolayer, nor do they provide any specific detail about the drug location in reference to the surfactant molecules. The intrinsic drug orientation was described earlier in Section 2.3.4. Figure 4 shows the drug orientation distributions as a function of distance from the intrinsic surface for the monolayer simulations. One prominent difference between these distributions is that T samples a wider range of orientations compared to TP and TE, as shown by the relatively flat distributions across $\cos(\theta)$ in Figures 4a and 4b. Additionally, the T molecules occupy both the C_{1-4} and C_{5-8} regions in the monolayers with just a single T molecule. However, as more T molecules are added to the monolayers, the C_{5-8} region becomes more densely populated and the drug molecules also tend to reorient themselves such that they are perpendicular to the monolayer/water interface. In doing so, the majority of the T molecules orient with their O_1 and O_2 atoms are nearest the water and the vacuum region, respectively. While there is a smaller popultion of T molecules which are oriented ($\cos(\theta) \sim 0.9$) with their O_2 atoms nearest the water and the O_1 nearest the vacuum region.

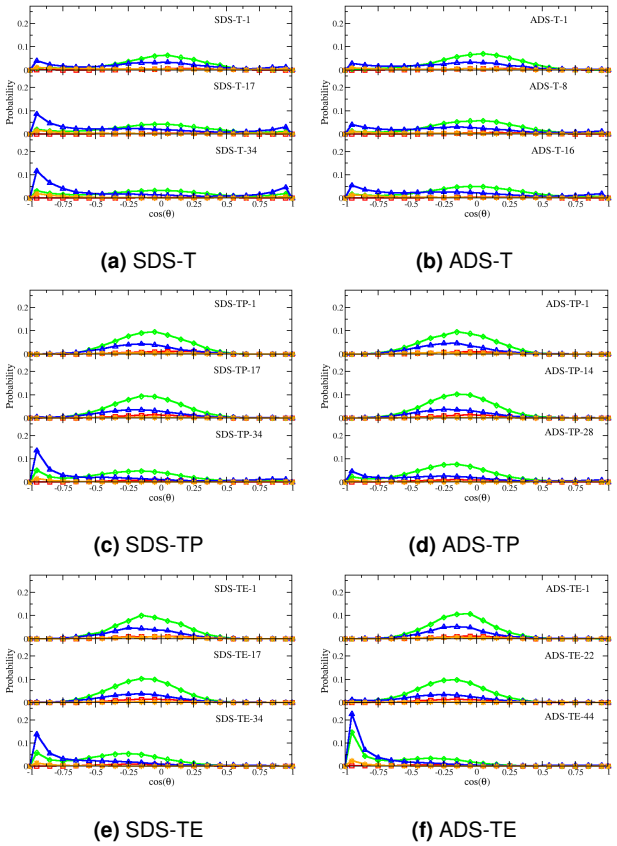

Fig. 4 Intrinsic drug orientation distributions for the various different monolayer simulations. The monolayer system is labelled in each subplot. For all plots, the colours red, green, blue and orange represent the Headgroup, C_{1-4}, C_{5-8} and C_{9-12} regions respectively.(Note: The errors of these measurements are smaller than the size of the symbols used to represent them.)

The TP molecules strongly populate the C_{1-4} region of the monolayers, with a distribution centred at $\cos(\theta) \sim -0.13$ which corresponds to the TP molecules being oriented approximately in the *x-y* plane within this part of the monolayer. This is shown

clearly by the prominent green curves in Figures 4c and 4d. When TP is present in excess of the ratio of drug to surfactant found in micelles, the C_{5-8} region becomes more populated and exhibits peaks at $\cos(\theta) = -0.9$ corresponding to the TP molecules reorienting themselves such that the O_1 atoms (see Figure 1) are nearest the water in a similar way as for the T molecules.

The TE molecules show very similar distibutions of their orientations as is observed with the TP molecules. Specifically, the TE also occupy the C_{1-4} region and exhibit the same shift of population to the C_{5-8} region when there is excess drug present within the monolayers.

The rationale of these results comes from considering the competing forces at play within these monolayers. Each of the testosterone-based compounds have oxygen atoms O_1 and O_2 on either end of the molecule which are capable of forming hydrogen bonds with the water in the solvent phase. Therefore, orientations with the drug molecule being parallel to the *x*-*y* plane will be preferable. This ensures that hydrogen bonds can be formed between water molecules and these polar sites within the drug molecule. For these hydrogen bonds to be formed, the drug molecule must have some contact with water molecules which explains why they sit in the C_{1-4} region which is close to the headgroups and approximately the location of the interface with the solvent phase within the monolayer, but also allows for the drugs to form hydrophobic contacts. As more drug molecules are packed into the monolayers within a fixed surface area, the packing of the monolayer chains and drugs causes the drug molecules to reorient themselves such that they are approximately parallel to the *z*-axis, and in doing so the centre of the molecule is moved deeper into the monolayer. The mechanism behind this reorientation is two-fold. First, the steric interactions become significant as packing increases. Second, by reorienting the drug in this manner interactions can be formed between the water molecules and one end of the drug molecule which most strongly prefers interactions with water. For all of the testosterone-based drug molecules, there is a preference for the drug molecules to orient such that the O_1 atoms interact with the water in the solvent phase. For the testosterone drugs, there is a smaller but significant population of drug molecules which orient such that O_2 interacts with the water, but there is no such population for the TE or TP molecules which have hydrophobic hydrocarbon chains attached to the O_2 atoms that would cause this end of the molecule to be decidedly less favourable to be in contact with water.

3.3 Monolayer structure

As the testosterone-based compounds are found to reside in the region of the monolayer where the hydrocarbon tail joins the DS^- headgroup, it is predictable that the addition of testosterone-based compounds has an appreciable effect on the structural properties of surfactant monolayers. By developing a detailed understanding of this, the rationale behind enhancing the solubility of poorly soluble drug compounds within surfactant aggregates can be improved for formulations in the future. A summary of the structural properties of the SDS and ADS monolayers can be found in Tables 1 and 2, respectively. Additionally, the surfactant chain tilt angle θ_t and the headgroup tilt angle θ_h were calculated for all monolayer systems and their probability distributions are shown in Figure 5, and the mean values of these angles have been reported in Tables 3 & 4.

Table 1 Structural properties of SDS monolayers containing T, TP and TE.

System	d_{tail} (Å)	d_{head} (Å)	Roughness (Å)	n_{H_2O} (#/Å^{-2})
SDS-T-1	7.8 ± 0.2	2.2 ± 0.04	2.7 ± 0.2	0.16
SDS-T-17	9.0 ± 0.2	2.2 ± 0.04	2.6 ± 0.2	0.13
SDS-T-34	9.9 ± 0.2	2.2 ± 0.04	2.3 ± 0.2	0.11
SDS-TP-1	7.9 ± 0.2	2.2 ± 0.03	2.7 ± 0.2	0.15
SDS-TP-17	9.0 ± 0.2	2.2 ± 0.03	2.4 ± 0.2	0.12
SDS-TP-34	10.1 ± 0.2	2.2 ± 0.03	2.5 ± 0.2	0.10
SDS-TE-1	7.8 ± 0.3	2.2 ± 0.03	2.6 ± 0.2	0.15
SDS-TE-17	9.2 ± 0.2	2.2 ± 0.03	2.4 ± 0.2	0.11
SDS-TE-34	10.4 ± 0.2	2.2 ± 0.03	2.5 ± 0.2	0.10

Table 2 Structural properties of ADS monolayers containing T, TP and TE.

System	d_{tail} (Å)	d_{head} (Å)	Roughness (Å)	n_{H_2O} (#/Å^{-2})
ADS-T-1	7.9 ± 0.2	2.2 ± 0.03	2.5 ± 0.2	0.10
ADS-T-8	8.3 ± 0.2	2.2 ± 0.03	2.5 ± 0.2	0.09
ADS-T-16	8.9 ± 0.2	2.2 ± 0.03	2.4 ± 0.2	0.08
ADS-TP-1	7.9 ± 0.2	2.2 ± 0.03	2.6 ± 0.2	0.10
ADS-TP-14	8.7 ± 0.2	2.2 ± 0.03	2.3 ± 0.2	0.07
ADS-TP-28	9.7 ± 0.2	2.2 ± 0.03	2.3 ± 0.2	0.05
ADS-TE-1	7.9 ± 0.2	2.2 ± 0.03	2.5 ± 0.2	0.10
ADS-TE-22	9.6 ± 0.2	2.2 ± 0.03	2.3 ± 0.2	0.06
ADS-TE-44	11.2 ± 0.2	2.2 ± 0.03	2.4 ± 0.2	0.04

The thickness of the monolayer headgroup region, d_{head} is equal to 2.2 Å for all of the systems. Meanwhile, there is a small shift in the distributions of the head group tilt angle θ_t toward smaller angles with increasing amounts of drug molecules within a monolayer, but the net effect on the mean value of this angle is generally insignificant. The distributions of θ_t also become more narrow with increasing amounts of drug. This indicates that as the effective area per molecule in the monolayer reduces so do the fluctuations in the conformations that the headgroup takes. Neither changing the counterion species, nor the presence of the different testosterone-based compounds, has any significant effect on the conformation of the headgroups, which is consistent with the results presented previously showing the drugs do not interact strongly with the headgroup regions.

The addition of drug molecules results in a significant effect on the structure of the hydrocarbon tails of the DS^- surfactants. From Tables 1 & 2, it is clear that there is a consistent trend of increasing hydrocarbon tail thickness with increasing amounts of drug molecules present in the monolayers. Additionally, Fig. 5 shows that the distributions of the tail tilt angle θ_t shift towards smaller angles as the amount of drug molecules interacting with the monolayer is increased. This trend is also confirmed by the monotonically decreasing mean values of these distributions with the addition of more drug molecules as shown in Tables 3 &

4. Since the monolayers are always held at a constant surface area, the area per surfactant molecule is reduced as more drug molecules are added to the monolayer. Therefore the surfactant tails are restricted to more rigid configurations which results in an increase of the effective tail length.

Table 3 Average head group (θ_h) and tail (θ_t) tilt angles of SDS monolayers containing T, TP and TE.

System	θ_h (°)	θ_t (°)
SDS-T-1	44.8 ± 23.2	44.3 ± 20.8
SDS-T-17	41.8 ± 22.1	37.1 ± 19.4
SDS-T-34	38.4 ± 20.8	30.4 ± 16.5
SDS-TP-1	44.8 ± 23.1	39.5 ± 18.8
SDS-TP-17	41.8 ± 21.7	33.2 ± 16.3
SDS-TP-34	38.0 ± 20.4	26.4 ± 14.5
SDS-TE-1	44.8 ± 23.1	43.9 ± 20.8
SDS-TE-17	41.0 ± 21.3	35.1 ± 17.5
SDS-TE-34	36.6 ± 19.8	27.0 ± 14.7

Table 4 Average head group (θ_h) and tail (θ_t) tilt angles of ADS monolayers containing T, TP and TE.

System	θ_h (°)	θ_t (°)
ADS-T-1	44.7 ± 23.1	44.1 ± 20.7
ADS-T-8	43.3 ± 22.6	41.0 ± 20.2
ADS-T-16	42.1 ± 22.2	37.6 ± 19.2
ADS-TP-1	44.4 ± 23.0	43.7 ± 20.8
ADS-TP-14	42.4 ± 22.0	38.3 ± 18.7
ADS-TP-28	39.1 ± 20.6	31.6 ± 16.1
ADS-TE-1	44.7 ± 23.2	43.9 ± 20.8
ADS-TE-22	39.6 ± 20.7	32.6 ± 16.4
ADS-TE-44	34.2 ± 19.1	23.3 ± 13.4

The roughness was also quantified for all systems by calculating RMSD values, which generally yielded values in the range of 2 Å to 3 Å (see Tables 1 & 2). This shows that the addition of testosterone-based compounds to the monolayers does not significantly compromise structural stability. Therefore the stability of any ADS or SDS monolayer should not be affected by the encapsulation of these testosterone-based compounds.

We have also calculated the surface tension for each simulated system, and the results are shown in the SI. The first thing to notice is that the surface tension for the SDS and ADS monolayers without any drug present are the same within the reported error bars, so the counter ion has no significant effect on the surface tension of these monolayers. Additionally, the results show that the surface tension of the monolayers are unaffected by the presence of the testosterone (TO) in either monolayer. In the SDS-TE and SDS-TP systems, we observe that when the ratio of drug to surfactant is less than or equal to that found in micelles experimentally, the presence of the drug has little effect on the surface tension of the monolayers. However when TE and TP are present at drug to surfactant ratios that are twice the ratio found in micelles, we observe a significant decrease in surface tension for the SDS monolayers. This observation is in agreement with our recent experiments of the same systems over a number of concentrations of drugs in which we observed that there is a decrease in the surface tension for SDS monolayers with an area per molecule of ~ 48 Å^2 without drug (~ 38 mN/m) and the same SDS monolayers with enough TE to saturate the monolayer (~ 29 mN/m) [48]. In the ADS monolayers, TP has no significant effect on the measured surface tension of any of the systems we studied. Whereas, TE decreases the surface tension of the ADS monolayer when it is present at a twice the drug to surfactant ratio found in micelles. Therefore, in all of the systems in which we observed drug molecules accumulating in the hydrocarbon tail regions of the surfactant monolayers, which would be indicative of the surface being saturated, we also observe that the presence of the drugs cause a decrease in the surface tension of the monolayer.

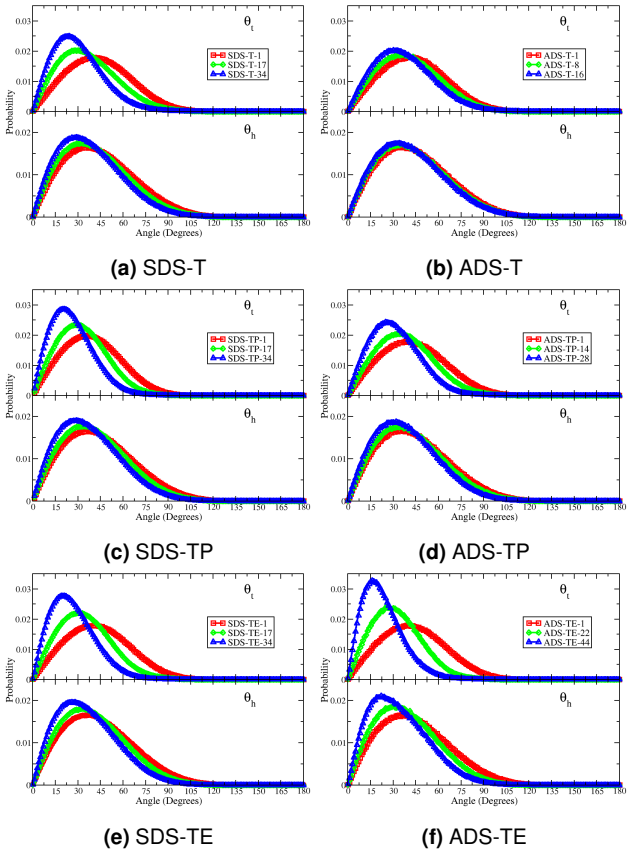

Fig. 5 Plots showing probability distributions of surfactant chain tilt, θ_t, and headgroup tilt, θ_h, angles for all monolayer simulations. The plots correspond to the various different monolayer simulations reported, as described by the legends. (Note: The errors of these measurements are smaller than the size of the symbols used to represent them.)

3.4 Effect of testosterone-based compounds on interactions with the solvent phase

While the drug molecules do not appear to interact with the surfactant head groups, the effect of the presence of the drug molecules on the interactions of the DS^- headgroups with water and the counter ions has been investigated to see if there is any significant change. The distributions of the hydration number around the surfactant head groups have been determined and are presented in the SI. The distributions of the hydration number for each monolayer exhibit unimodal distributions centred

around the mean value. The mean hydration number of each monolayer simulation is shown in Tables 5 & 6. Comparing these values reveals that the SDS monolayers are more hydrated than ADS, for example in the simulations with a single drug molecule present the hydration decreases from ~ 12.4 H_2O/molecule for the SDS monolayers to ~ 9.3 H_2O/molecule for ADS monolayers. The probability distributions do not change drastically when the number of drug molecules per monolayer is varied, however the mean hydration number does decrease slightly as the number of drug molecules per monolayer is increased. Once again, the counterion species seems to be the dominant factor in determining hydration.

Also, the distribution of the number of cations bound to the DS^- headgroup has been used to investigate any effect that the presence of the drug molecules may have on interactions with the ions. The average number of ions bound to the DS^- headgroup in each system is reported in Tables 5 & 6, and these values show that there are more $NH_3{}^+$ ions bound per headgroup than Na^+ ions, which is consistent with the findings in our previous study of the interaction of different ions with the DS^- headgroup[26]. While the value of the average number of ions bound to the headgroup increases with an increase in the number of drug molecules in the monolayer, the change is not significant. Therefore it seems that the presence of drugs has very little effect on the properties of the interfaces between the monolayers and the solvent phase.

Table 5 Average number of first neighbour water molecules and Na^+ ions around the S atom in the SDS headgroup for the monolayers containing T, TP and TE.

System	$n^{hg}_{H_2O}$	$n^{hg}_{Na^+}$
SDS-T-1	12.4 ± 2.2	0.90 ± 0.84
SDS-T-17	12.0 ± 2.3	0.95 ± 0.87
SDS-T-34	11.7 ± 2.3	0.99 ± 0.88
SDS-TP-1	12.4 ± 2.2	0.92 ± 0.86
SDS-TP-17	11.9 ± 2.3	0.95 ± 0.86
SDS-TP-34	11.4 ± 2.4	0.99 ± 0.86
SDS-TE-1	12.4 ± 2.2	0.94 ± 0.85
SDS-TE-17	11.8 ± 2.3	0.97 ± 0.85
SDS-TE-34	11.4 ± 2.4	1.01 ± 0.88

Table 6 Average number of first neighbour water molecules and $NH_3{}^+$ ions around the S atom in the ADS headgroup for the monolayers containing T, TP and TE.

System	$n^{hg}_{H_2O}$	$n^{hg}_{NH_3^+}$
ADS-T-1	9.3 ± 2.2	1.38 ± 0.96
ADS-T-8	9.2 ± 2.2	1.39 ± 0.96
ADS-T-16	9.1 ± 2.3	1.39 ± 0.96
ADS-TP-1	9.3 ± 2.2	1.38 ± 0.96
ADS-TP-14	9.1 ± 2.2	1.39 ± 0.94
ADS-TP-28	8.7 ± 2.3	1.44 ± 0.95
ADS-TE-1	9.4 ± 2.2	1.38 ± 0.96
ADS-TE-22	8.8 ± 2.3	1.43 ± 0.95
ADS-TE-44	8.3 ± 2.4	1.50 ± 0.96

3.5 Hydration of testosterone-based compounds

While the drug molecules have been observed to change their orientation within the monolayers as more drugs are present, there is most probably an effect on the interaction of the drug molecules with water molecules and the ions in solution. Therefore, once again, the number of nearest neighbour water molecules and ions (Na^+ in the SDS systems and NH_3^+ in the ADS systems) have been determined around each oxygen in the different testosterone-based compounds, and then the probability distribution of having a certain number of water molecules and ions around each oxygen was determined. These probability distributions, which are displayed as histograms and are shown in the SI, exhibit unimodal distributions in each case.

Table 7 shows the average number of nearest neighbour water molecules around each of the oxygen atoms in the testosterone-based compounds in both the SDS and ADS monolayers. From these values, it is clear that there is a general trend in which the testosterone-based compounds in the ADS monolayers are more dehydrated than when they are in SDS monolayers. While the drugs do not interact with the headgroups of the monolayers, they do interact with the ions in solution, and from the distributions shown in the SI, it is clear that the NH_3^+ ions in the ADS systems interact more with the oxygens in the testosterone-based compounds than the Na^+ ions in the SDS systems do. As was shown with their interactions with the DS^- headgroups in a previous publication[26], the NH_3^+ ions are able to form hydrogen bonds with the oxygens (in particular O_1 and O_3, as shown in Fig. 1) and therefore more directly compete with water for interactions with these atoms, which the Na^+ ions do not.

The trends of the hydration numbers for each of the different testosterone-based compounds in the SDS monolayers and in the ADS monolayers are similar. For example, in the case of testosterone (T) in both the monolayers, the average hydration numbers are not significantly affected by increasing the number of drugs in the monolayers. In all systems the hydration of both the O_1 and O_2 atoms is approximately the same. When there is a single testosterone molecule in the monolayers, this is due to them most probably being oriented parallel to the interface with the water (as shown in Figs. 4a & 4b), so that both oxygens can interact with interfacial water molecules. The orientational preferences of the drugs in the two monolayers are reflected in the number of first neighbour water molecules around the O_1 and O_2 atoms in the testosterone molecules. In the ADS monolayers, the number of water molecules around the two oxygen atoms remains more or less constant with the number of drug molecules within the monolayers as they always prefer to be parallel to the interface with the water. While for the drugs in SDS, the number of first neighbour water molecules around O_1 becomes increasingly larger than that found around the O_2 atoms as the number of drug molecules increases and the drug molecules increasingly prefer to orient such that the O_1 atoms are near the water and the O_2 atoms are close to the vacuum region.

In the ADS monolayers, the hydration of the testosterone propionate (TP) molecules does not show any significant change with an increasing number of drugs present in the monolayer. This

hydration behaviour is consistent with the fact that the preferred orientation of the TP molecules in the ADS monolayers is such that the molecule is parallel to the water interface, independent of the number of drugs present (see Fig. 4d). Whereas, in the SDS monolayers, the hydration of the O_1 atom remains approximately constant independent of the number of drug molecules present. However, the O_2 and O_3 atoms dehydrate by approximately the same amount with increasing amounts of drug in the monolayer ($\sim$10% for 17 TP molecules and $\sim$40% for 34 TP molecules). This dehydration is a result of the TP molecules reorienting such that the end of the molecule containing the O_2 and O_3 atoms and the hydrocarbon chain moves into the vacuum region of the system with increasing number of drugs present (see Fig. 4c).

The hydration of the O_1, O_2 and O_3 atoms in the testosterone enanthate (TE) molecules follow the same trends with increasing number of drug molecules in both of the monolayers. The number of first neighbour water molecules around the O_1 atoms slightly increases as the number of drug molecules increases. Meanwhile the number of hydrating of water molecules around both the O_2 and O_3 atoms decreases significantly ($>$ 50% for the systems which have a larger drug to surfactant ratio than found in a micelle) as the number of drug molecules increases. This trend is once again consistent and seemingly a result of the fact that the TE molecules reorient from being parallel to the water interface to being perpendicular to the water interface with the O_1 atom nearest the water as the number of drug molecules increase (see Figs. 4e & 4f).

Table 7 Average number of first neighbour watr molecules around oxygen atoms of the testosterone-based compounds (O1, O2, & O3 as seen in Fig. 1) in the various SDS and ADS monolayer systems.

System	$n_{H_2O}^{O_1}$	$n_{H_2O}^{O_2}$	$n_{H_2O}^{O_3}$
SDS-T-1	2.2 ± 0.8	2.1 ± 0.9	—
SDS-T-17	2.0 ± 1.4	1.9 ± 1.7	—
SDS-T-34	1.9 ± 1.5	1.5 ± 1.7	—
SDS-TP-1	2.6 ± 0.7	0.8 ± 0.4	4.0 ± 1.0
SDS-TP-17	2.5 ± 1.3	0.7 ± 0.7	3.7 ± 1.9
SDS-TP-34	2.5 ± 1.6	0.5 ± 0.6	2.3 ± 2.3
SDS-TE-1	2.6 ± 0.7	0.8 ± 0.4	4.1 ± 1.0
SDS-TE-17	2.6 ± 1.3	0.7 ± 0.7	3.5 ± 1.8
SDS-TE-34	2.8 ± 1.6	0.4 ± 0.6	2.0 ± 2.0
ADS-T-1	1.3 ± 0.5	1.3 ± 0.7	—
ADS-T-8	1.2 ± 0.9	1.3 ± 1.1	—
ADS-T-16	1.1 ± 0.9	1.3 ± 1.2	—
ADS-TP-1	1.3 ± 0.4	0.8 ± 0.4	1.6 ± 0.7
ADS-TP-14	1.2 ± 0.8	0.8 ± 0.8	1.6 ± 1.3
ADS-TP-28	1.1 ± 0.9	0.7 ± 0.7	1.3 ± 1.3
ADS-TE-1	1.3 ± 0.5	0.7 ± 0.4	1.6 ± 0.8
ADS-TE-22	1.4 ± 1.0	0.7 ± 0.7	1.5 ± 1.3
ADS-TE-44	1.7 ± 1.2	0.3 ± 0.6	0.6 ± 1.0

4 Discussion

A series of MD simulations investigating the interactions between SDS and ADS monolayers and three different testosterone-based compounds (testosterone (T), testosterone propionate (TP) and testosterone enanthate (TE)) were conducted to show how the structural and interfacial properties of the monolayer are affected by changing the number of drug molecules present per monolayer, and the chemical nature of the surfactant counterions and the testosterone-based compounds.

The results show that the encapsulation and resultant structure of the molecules within the monolayers are dependent upon both the chemistry of the drugs and the counterion used to neutralise the DS^- monolayers. The counterion affects the properties related to hydration of the monolayers and the drugs. The chemistry of the drug plays a role in the preferred orientation of the drug molecule within the monolayers, particularly once the number of drugs within the monolayer is above the saturation level. Finally, the number of drugs within the monolayers affect the structure of the monolayer, the position and orientation of the drug molecules within the monolayer and the amount of water found within the monolayer.

The interfacial water structure in the SDS monolayer systems includes a layer of water molecules which are seemingly well ordered, whereas the water near the ADS monolayers show no such ordering. When investigating the hydration of the surfactant headgroups, the SDS monolayers were found to be significantly more hydrated than the ADS monolayers, which is consistent with previous findings that the NH_3^+ ions compete with water when binding to the DS^- headgroups, and therefore reduce the number of nearest neighbour water molecules[26]. However, increasing the number of drug molecules in the monolayer only minimally affects the surfactant headgroup hydration, which decreased slightly as the number of drug molecules present per monolayer increased.

In addition to reducing the hydration of the headgroups of the DS^- molecules, the NH_3^+ ions also reduce the amount of water that penetrates the monolayers when compared to that found when Na^+ ions are present. The amount of water that penetrates the ADS monolayers is approximately 50% smaller than that which penetrates the SDS monolayers. Additionally, in each monolayer, the amount of water that penetrates the monolayer reduces as the number of drug molecules that are present within the monolayers, as there is more steric hinderance to the diffusion of water.

The monolayer structural properties revealed that the monolayer headgroup thickness, d_{head}, remains constant in every monolayer system reported. However, the thickness of the hydrocarbon tail region, d_{tail}, increases as more drug molecules are added to the monolayer due to packing constraints. Distributions of the surfactant chain tilt, θ_t, and headgroup tilt angles, θ_h, shift towards smaller values as more drug molecules are added to the monolayers, an effect which is coupled with the observation of increased monolayer thickness. These trends are consistently observed independent of the chemistry of the testosterone-based compounds.

The location and orientation of the testosterone-based molecules within the different monolyers vary with the chemistry of the drug molecules and the number of each molecule in the monolayer; however there are some general trends that are observed in the various systems. When the number of the

drug molecules is at or less than the amount required to saturate the monolayer, the drug molecules prefer to reside within the monolayer in the C_{1-4} region with an orientation such that the molecule is parallel to the water interface. When the drug to surfactant ratio is greater than or equal to that found in micelles, the centre of the drug molecules are found to be located deeper into the hydrophobic chains of the surfactants and then they orient themselves such that they are nearly perpendicular to the interface with the water interface such that the O_1 atoms in the drug molecules are closest to the water. In doing so, the O1 oxygen can hydrogen bond with the water molecules and the hydrocarbon tail is able to interact with the hydrocarbon tails of the surfactant when the packing increases within the monolayer. The only systems that differs from these trends are the ones with testosterone (T) molecules. In the systems with T molecules, there is a large population which orient with the O_1 atoms nearest the water interface, and there is also a population, which is smaller in number, of drug molecules that oriented with the O_2 atom closest to the water.

The hydration of the oxygens within the drug molecules is affected by the rotation of the molecules within the monolayers. Therefore while there is a general reduction in the hydration of the oxygens in the drug molecules as the number of drugs in a monolayer increases, the degree to which the hydration is decreased around the O_2 (and O_3) atom(s) of the drug molecule increases with increasing hydrocarbon chain length (T $>$ TP $>$ TE). Also the drug molecules in the ADS monolayers generally show that they have roughly half of the number of hydrating water molecules around their oxygens as compared to the drug molecules in the SDS monolayers. This results from the fact that there is approximately half as much water that penetrates into the ADS monolayers as compared to the SDS monolayers.

To conclude, we have provided direct evidence of how subtle changes in the chemistry of drug molecules and the surfactant molecules used to encapsulate them can have a significant effect on the structure of the resulting aggregate and therefore the amount of drug that can be encapsulated. One example of this phenomena in practice is the recent experimental work showing that ADS micelles have a poorer solubilisation capacity for encapsulating testosterone derivatives than SDS micelles despite being having a larger aggregation number and lower hydration[49]. Our results suggest that this is due to the testosterone-based compounds being significantly dehydrated within the aggregates of ADS as compared to when they are encapsulated within aggregates of SDS.

Acknowledgements

D. T. A. and C. D. L. thank the EPSRC for the GTA studentship which funds D. T. A.'s research. Y. S. and M. J. L. thank the GET-Fund (Ghana Education Trust Fund) for funding the Ph.D. studentship of Y. S. Additionally, D. T. A. and C. D. L. acknowledge the stimulating research environment provided by the EPSRC Centre for Doctoral Training in Cross-Disciplinary Approaches to Non-Equilibrium Systems (CANES, EP/L015854/1). Also, C. D. L. and N. D. thank the Faculty of Natural and Mathematical Sciences and the Department of Physics at King's College London for funding a summer internship for N. D. that allowed her to participate in this research. It is through our membership within the UK HPC Materials Chemistry Consortium, which is funded by the Office of Science and Technology through the EPSRC High End Computing Programme (Grant No. EP/L000202), that we were able to use the facilities of ARCHER, the UK National Supercomputing Service (http://www.archer.ac.uk), to carry out aspects of this work. Also, some of the simulations were conducted using computational time on the MareNostrum supercomputer, which was generously provided by the Barcelona Supercomputing Center through a grant from Red Española de Supercomputación.

Conflict of interest

There are no conflicts to declare.

References

1 D. T. Allen, Y. Saaka, M. J. Lawrence and C. D. Lorenz, *J. Phys. Chem. B*, 2014, **118**, 13192–13201.
2 C. J. Drummond and C. Fong, *Curr. Opin. Colloid Interface Sci.*, 2000, **4**, 449–456.
3 A.-L. Fameau, A. Arnould and A. SaintJalmes, *Curr. Opin. Colloid Interface Sci.*, 2014, **19**, 471 – 479.
4 L. I. Schramm, *Emulsions, Foams and Suspensions: Fundamentals and Applications*, WILEY-VCH Verag GmbH & Co. KGaA, 2005.
5 S. Paria and K. C. Khilar, *Adv. Drug Delivery Rev.*, 2000.
6 M. J. Lawrence and G. D. Rees, *Adv. Colloid Interface Sci.*, 2000.
7 B. E. Rabinow, *Nat. Rev. Drug Discovery*, 2004.
8 B. Mishra, B. B. Patel and S. Tiwari, *Nanomed. Nanotechnol. Bio. Med.*, 2010.
9 L. Cohen, M. Martin, F. Soto, F. Trujillo and E. Sanchez, *J. Surfactants Deterg.*, 2016, **19**, 219–222.
10 T. S. Banipal, H. Kaur, A. Kaur and P. K. Banipal, *Food chemistry*, 2016, **190**, 599–606.
11 S. Kumar and A. Mandal, *Appl. Surf. Sci.*, 2016, **372**, 42–51.
12 L. D. Rhein, M. Schlossman, A. O'Lenick and P. Somasundaran, *Surfactants in Personal Care Products and Decorative Cosmetics*, CRC Press, 3rd edn., 2006.
13 C. Yang, Z. Shen, L. Wu, H. Tang, L. Zhao, F. Cao and H. Sun, *J. Molec. Model.*, 2017, **23**, 211.
14 A. Phan, T. Bui, E. Acosta, P. Krishnamurthy and A. Striolo, *Phys. Chem. Chem. Phys.*, 2016, **18**, 24859–24871.
15 T. Bui, A. Phan, D. Monteiro, Q. Lan, M. Ceglio, E. Acosta, P. Krishnamurthy and A. Striolo, *Langmuir*, 2017, **33**, 2263–2274.
16 C. O. Rangel-Yagui, A. Pessoa Jr. and L. C. Tavares, *J. Pharm. Pharmaceut. Sci.*, 2005.
17 B. Maity, A. Chatterjee, S. A. Ahmed and D. Seth, *J. Phys. Chem. B*, 2015, **119**, 3776–3785.
18 H. Yan, P. Cui, C. B. Liu and S. L. Yuan, *Langmuir*, 2012, **28**, 4931–4938.
19 M. Schwarze, I. Volovych, S. Wille, L. Mokrushina, W. Arlt and R. Schomäcker, *Ind. Eng. Chem. Res.*, 2012, **51**, 1846–1852.

20 S. Storm, S. Jakobtorweihen, I. Smirnova and A. Z. Panagiotopoulos, *Langmuir*, 2013, **29**, 11582–11592.

21 X. Liang, M. Marchi, C. Guo, Z. Dang and S. Abel, *Langmuir*, 2016, **32**, 3645–54.

22 S. Soleimanzadegan, H. Farsi and F. Ebrahimi, *J. Molec. Struct.*, 2015, **1079**, 494–501.

23 S. Karaborni, N. M. van Os, K. Esselink and P. A. J. Hilbers, *Langmuir*, 1993, **9**, 1175–1178.

24 D. Yordanova, E. Ritter, T. Gerlach, J. H. Jensen, I. Smirnova and S. Jakobtorweihen, *J. Phys. Chem. B*, 2017, **121**, 5794–5809.

25 Y. Wei, H. Wang, G. Liu, Z. Wang and S. Yuan, *RSC Adv.*, 2016, **6**, 84090–84097.

26 D. T. Allen, Y. Saaka, M. J. Lawrence and C. D. Lorenz, *Phys. Chem. Chem. Phys.*, 2016, **18**, 30394–30406.

27 A. P. Dabkowska, L. E. Collins, D. J. Barlow, R. Barker, S. E. McLain, M. J. Lawrence and C. D. Lorenz, *Langmuir*, 2014, **30**, 8803–8811.

28 C. D. Lorenz and A. Travesset, *Langmuir*, 2006, **22**, 10016–10024.

29 D. Hu, A. Mafi and K. C. Chou, *J. Phys. Chem. B*, 2016, **120**, 2257–2261.

30 K. J. Schweighofer, U. Essmann and M. Berkowitz, *J. Phys. Chem. B*, 1997, **101**, 3793–3799.

31 P. A. Kralchevsky, K. D. Danov, , G. Broze and A. Mehreteab, *Langmuir*, 1999, **15**, 2351–2365.

32 G. Hantal, L. B. Pártay, I. Varga, P. Jedlovszky and T. Gilányi, *J. Phys. Chem. B*, 2007, **111**, 1769–1774.

33 J. J. Giner Casares, L. Camacho, M. T. Martín-Romero and J. J. López Cascales, *ChemPhysChem*, 2008, **9**, 2538–2543.

34 H. Yan, X.-L. Guo, S.-L. Yuan and C.-B. Liu, *Langmuir*, 2011, **27**, 5762–5771.

35 M. Chen, X. Lu, X. Liu, Q. Hou, Y. Zhu and H. Zhou, *Langmuir*, 2014, **30**, 10600–10607.

36 M. Chen, X. Lu, X. Liu, Q. Hou, Y. Zhu and H. Zhou, *J. Phys. Chem. C*, 2014, **118**, 19205–19213.

37 T. Zhao, G. Xu, S. Yuan, Y. Chen and H. Yan, *J. Phys. Chem. B*, 2010, **114**, 5025–5033.

38 L. Shi, N. R. Tummala and A. Striolo, *Langmuir*, 2010, **26**, 5462–5474.

39 J. V. N. Ferreira, T. M. Capello, L. J. A. Siqueira, J. H. G. Lago and L. Caseli, *Langmuir*, 2016, **32**, 3234–3241.

40 E. D. Estrada-López, E. Murce, M. P. P. Franca and A. S. Pimentel, *RSC Adv.*, 2017, **7**, 5272–5281.

41 S. Ortiz-Collazos, E. D. Estrada-López, A. A. Pedreira, P. H. Picciani, O. N. Oliveira and A. S. Pimentel, *Colloids Surf. B: Biointerfaces*, 2017, **158**, 689–696.

42 U. K. Basak, A. Datta and D. Bhattacharyya, *Colloids Surf. B: Biointerfaces*, 2015, **132**, 34–44.

43 B. Korchowiec, J. Korchowiec, M. Orlof-Naturalna, J.-B. R. de Vains and E. Rogalska, *Colloids and Surfaces B: Biointerfaces*, 2016, **145**, 777–784.

44 R. Bradbury, J. Penfold, R. K. Thomas, I. M. Tucker, J. T. Petkov and C. Jones, *Langmuir*, 2013, **29**, 3361–3369.

45 R. Bradbury, J. Penfold, R. K. Thomas, I. M. Tucker, J. T. Petkov and C. Jones, *J. Colloid Interface Sci.*, 2016, **461**, 352–358.

46 J. R. Lu, , Z. X. Li, R. K. Thomas, B. P. Binks, D. Crichton, , P. D. I. Fletcher, J. R. McNab and J. Penfold, *J. Phys. Chem. B*, 1998, **102**, 5785–5793.

47 J. R. Lu, T. J. Su, M. J. Lawrence, D. J. Barlow, W. Warisnoicharoen and T. Zuberi, *J. Phys. Chem. B*, 1999, **103**, 4638–4648.

48 Y. Saaka, D. T. Allen, Y. Luangwitchajaroen, Y. Shao, R. A. Campbell, C. D. Lorenz and M. J. Lawrence, *Soft Matter*, 2017, submitted.

49 Y. Saaka, *Ph.D. Thesis*, University of London, 2016.

50 L. Martinez, R. Andrade, E. G. Birgin and J. M. Martinez, *J. Comput. Chem.*, 2009, **30**, 2157–2164.

51 T. Kawai, H. Kamio, T. Kondo and K. Kon-No, *J. Phys. Chem. B*, 2005, **109**, 4497–4500.

52 S. Plimpton, *J. Comput. Phys.*, 1995, **117**, 1–19.

53 K. Vanommeslaeghe, E. Hatcher, C. Acharya, S. Kundu, S. Zhong, J. Shim, E. Darian, O. Guvench, P. Lopes, I. Vorobyov and A. D. MacKerell Jr., *J. Comput. Chem.*, 2010, **31**, 671–690.

54 W. Yu, K. Vanommeslaeghe and A. D. MacKerell Jr., *J. Comput. Chem.*, 2012, **33**, 2451–2468.

55 J. B. Klauda, R. M. Venable, J. A. Freites, J. W. O'Connor, D. J. Tobias, C. Mondragon-Ramirez, I. Vorobyov, A. D. MacKerell Jr. and R. W. Pastor, *J. Phys. Chem. B*, 2010, **114**, 7830–7843.

56 R. W. Pastor and A. D. MacKerell Jr., *J. Phys. Chem. Lett.*, 2011, **2**, 1526–1532.

57 W. L. Jorgensen, J. Chandrasekhar, J. D. Madura, R. W. Impey and M. L. Klein, *J. Chem. Phys.*, 1983, **79**, 926–935.

58 W. I. Reiher, *Theoretical Studies of Hydrogen Bonding*, Ph.D. dissertation, Harvard University, 1985.

59 X. Tang, P. H. Koenig and R. G. Larson, *J. Phys. Chem. B*, 2014, **118**, 3864–3880.

60 D. T. Allen and C. D. Lorenz, *J. Mol. Model.*, 2017, **23**, 219.

61 T. Darden, D. York and L. Pedersen, *J. Chem. Phys.*, 1993, **98**, 10089–10092.

62 W. G. Hoover, *Phys. Rev. A*, 1985, **31**, 1695–1697.

63 J. P. Ryckaert, G. Ciccotti and H. J. C. Berendsen, *J. Comput. Phys.*, 1977, **23**, 327–341.

64 S. A. Pandit, D. Bostick and M. L. Berkowitz, *J. Chem. Phys.*, 2003, **119**, 2199–2205.